Recombination efficiency of vacancies and self-interstitials in a concentrated AgZn alloy

M. Halbwachs* and J. Hillairet

Centre d'Etudes Nucléaires de Grenoble, Département de Recherche Fondamentale, Section de Physique du Solide, 85 X, 38041 Grenoble Cédex, France

(Received 31 July 1980)

A novel approach was devised for the determination of the recombination efficiency of vacancies and self-interstitials. It is based on the performance of anelasticity experiments to measure the rate at which directional order is established in ordering alloys. This method applies specifically to concentrated substitutional alloys. It is shown that it enables us to explore a wide temperature region above stage III, a domain in which data are scarce. Application to a Ag-30 at. % Zn solid solution is presented. Experiments were conducted during electron irradiation at a constant flux rate or after flux was suppressed. The recombination reaction constants were measured at a series of temperatures ranging between 200 and 350 K. The inferred capture radius is about six interatomic distances at the highest temperature examined, 340 K. Its variation with temperature is analyzed and discussed.

I. INTRODUCTION

For a long time, the interaction between vacancies and self-interstitials has been described by a phenomenological reaction radius, r_v, with the following meaning:

Whenever a mobile particle comes closer to its reaction partner than r_v, the annihilation reaction is assumed to take place instantaneously.

For larger separations, no interaction is considered and the motion of the migrating defect is treated as free isotropic continuum diffusion.

Recent refinements[1-3] include the drift term due to the existence of long-range interaction potentials mainly of elastic origin. It was shown that the concept of a reaction radius could be retained but in this scheme the recombination radius corresponds to the distance at which the potential energy equals the thermal energy of the diffusing defect. It becomes thereby temperature dependent. Thus, effects of temperature, as well as defect parameters and elastic properties of the matrix have to be taken into account in any analysis of the recombination behavior.

On the other hand the characteristics of the spontaneous recombination volume have been determined experimentally in a number of pure metals and dilute alloys, mostly with the help of electrical resistivity measurements, but the bulk of the investigation was performed at irradiation temperatures located below stage III. The present work was initiated to complement the available information by extending the measuring range to higher temperatures. A novel approach was used, based on the realization of anelasticity measurements, to follow the rate at which directional order is established in an ordering alloy and derive the recombination rate of point defects in conditions of permanent irradiation or after sudden suppression of flux.

This method is well suited to temperatures above stage III and enables us to explore a wide temperature region. In addition, it applies specifically to concentrated binary alloys for which only little data exist. Application to an Ag-30 at. % Zn alloy exposed to electron irradiation is presented in the following discussion. The recombination radius could be measured at a series of temperatures ranging between 200 and 340 K, that is, from about 0.2 to 0.35 melting temperature in K.

II. PRESENT AND FORMER APPROACHES TO THE RECOMBINATION VOLUME

The several experimental approaches to the recombination volume which can be used all involve the knowledge of other physical parameters as will be discussed in this section.

(1) At temperatures for which the created defects have no significant mobility, that is, below stage I, the determination of the spontaneous recombination volume is based on the study of the saturation behavior of defect production. Namely, at increasing defect concentrations, the existence of the recombination volumes associated with the Frenkel pairs causes a progressively decreased effective production rate. However, another effect is superimposed which results in the same trend. It originates in the occurrence of subthreshold energy transfers to atoms in the neighborhood of a preexisting stable Frenkel pair, which can induce its recombination. Then, the production rate of Frenkel pairs is given by[4]

$$\frac{dc}{dt}=\sigma_d\phi(1-v_r c)^2-\sigma_i\phi c \ . \tag{1}$$

c is their instantaneous atomic concentration at a flux rate ϕ. v_r is the recombination volume, in units of atomic volumes, and the σ's are the ap-

propriate cross sections for atomic displacements and induced recombination, respectively.

Essentially, resistivity measurements have been used to monitor the considered production rate of point defects. This type of work was conducted in several metals.[5-8] Nevertheless the two contributions, static recombination and induced recombination, could be separated in a few cases only in which they were found to be of about equal importance for the saturation behavior.[4] Now it is to be noted that the analysis of the resistivity damage curves yields only the product of the spontaneous recombination volume and the resistivity increment per unit defect concentration, ρ_F. Thus the choice for ρ_F is crucial and is a definite source of uncertainty in the determination of r_v. Incidently, the relevant recombination volume in the present case when both created species have no significant mobility is somewhat different in nature from the "capture" radius which is determined in conditions when one of the reaction partners is mobile as envisaged in the following.

(2) Recovery studies in the course of stage I bring direct information about the capture radius.[9] After close pair recombination is completed in substages I_A, I_B, and I_C, all the remaining interstitials migrate randomly through the lattice. However, by applying the diffusion theory of a three-dimensionally migrating interstitial, it is shown that a substantial fraction of them return to the recombination volume of their own vacancy giving rise to a substage I_D. The corresponding probability for interstitials deposited at a distance r_p of their native vacancy is r_v/r_p.[10] Thus the measurement of the fractional resistivity annealing in substage I_D yields the r_v/r_p value averaged over all nonclose Frenkel pairs. At sufficiently low defect concentrations, stages I_D and I_E are well separated, and $\langle r_v/r_p \rangle$ can be determined with good accuracy. However, the uncertainty in r_p is a serious limitation to the accurate derivation of r_v. In addition, application of the method is inherently restricted to a narrow temperature range.

(3) Another valuable approach to the recombination characteristics is the measure of the defect production rate at temperature above stage I but below stage III, that is, when the vacancies are still immobile. In this case, an interstitial which has been displayed from its own vacancy to a distance r_p larger than r_v can either return correlatedly to the recombination volume of its native vacancy as mentioned above or react with other lattice defects, which results in its annihilation with another vacancy or its trapping on an impurity atom. Consequently, the number of surviving Frenkel defects, vacancies, and trapped–interstitials is given at any instant during an irradiation in a flux ϕ by[11-13]

$$\frac{\partial c}{\partial t} = \sigma_m \left(1 - \left\langle \frac{r_v}{r_p} \right\rangle\right) \phi \frac{r_t c_t}{r_v c_v + r_t c_t}, \tag{2}$$

where σ_m is the displacement cross section for randomly migrating interstitials. c_t and r_t are the concentration and the capture radius of the impurity traps, respectively.

Again, as in the preceding cases, electrical resistivity measurements are usually used to monitor the damage rate. By integration of expression (2), one is led to

$$\left(\frac{\partial \Delta\rho}{\partial \phi}\right)^{-1} = \frac{1}{\sigma_m \left(1 - \left\langle \frac{r_v}{r_p} \right\rangle\right) \rho_F} \left(1 + \frac{\Delta\rho}{\rho_F C_t \frac{r_t}{r_v}}\right). \tag{3}$$

According to this expression, the temperature dependence of r_v/r_p and r_v/r_t can be obtained by measuring damage rates as a function of the irradiation-induced resistivity increase for different irradiation temperatures. Further, $\langle r_v/r_p \rangle$ can be evaluated if ρ_F and σ_m are known. However, as underlined by Lennartz *et al.*,[14] this determination is not accurate in the case of high-purity metals since the $(\partial\Delta\rho/\partial\phi)^{-1}$ against $\Delta\rho$ data obey Eq. (3) only at low defect concentrations. To avoid this difficulty dilute alloys were prefered, since it was verified experimentally that Eq. (3) was then obeyed in a wide range of concentrations and temperatures. However, the probability of correlated recovery is smaller in the alloy than in the host material as a result of the capture of part of the diffusing interstitials by the solute atoms.[10,15] By considering this effect and combining data analysis for pure metal and doped specimens, the recombination radii r_v can be obtained separately from the displacement distance r_p.[14] In copper, for instance, the capture radius at a vacancy r_v could be determined between 50 and 107 K.

In concentrated alloys kinetics of the radiation-induced atomic redistribution can be followed also by use of electrical resistivity. This type of experiment was performed, for instance, in Cu-Ni alloys to monitor the decomposition kinetics associated with the interstitialcy diffusion.[16] Comparison of the model calculation to the data give the recombination radius of the vacancy. It is to be noted that the temperature dependence of the recombination radius of the vacancy found in this case is much stronger than predicted by theory[1] or found in pure copper[17]; namely, it indicates an interaction energy inversely proportional to the distance between interstitial and vacancy.

4. The present experiments were conducted in conditions of permanent irradiation at tempera-

tures above stage III. Then the mobilities of both vacancies and self-interstitials have to be taken into account. The dynamic concentrations of point defects which are formed are adequately described by the two following equations[18-20]:

$$\frac{\partial c_v}{\partial t} = \sigma_d \epsilon \phi - Z c_i (c_v + c_{th})(\nu_i + \nu_v) - \rho c_v \nu_v ,$$
$$\frac{\partial c_i}{\partial t} = \sigma_d \epsilon \phi - Z c_i (c_v + c_{th})(\nu_i + \nu_v) - \rho c_i \nu_i . \quad (4)$$

They express the balance between the rate of production and the rate of elimination of vacancies and self-interstitials, respectively. Creation is due to flux ϕ, with efficiency equal to the product of the displacement cross section σ_d and the number ϵ of uncorrelated Frenkel pairs emitted by primary knock on. Annihilation occurs both by mutual recombination characterized by a recombination efficiency Z and by elimination at fixed sinks having a density ρ. c_{th} is the concentration of thermal vacancies. As a matter of fact the recombination efficiency Z is directly connected to the spontaneous recombination radius r_v. The appropriate relation is readily obtained by solving the diffusion equations in spherical coordinates for a system made of two defect species in equal number in zero flux.[21,22] The final expression is

$$\frac{\partial c_i}{\partial t} = \frac{\partial c_v}{\partial t} = -\frac{2\pi\sqrt{2}}{3} \frac{r_v}{\lambda} c_v c_i (\nu_i + \nu_v) , \quad (5)$$

where λ is the distance between first neighbors. Hence, as will be detailed below,

$$Z = \frac{2\pi\sqrt{2}}{3} \frac{r_v}{\lambda} . \quad (6)$$

In conditions when sinks can be neglected and the two defect species are produced in equal numbers, the balance equations restrict to one single expression

$$\frac{\partial c}{\partial t} = \sigma\epsilon\phi - Z c^2 (\nu_v + \nu_i) . \quad (7)$$

An implicit assumption is to neglect the concentration of thermal vacancies against the concentration of radiation defects. Integration of Eq. (7) leads to

$$c_v = c_i = \left(\frac{\sigma\epsilon\phi}{Z(\nu_v + \nu_i)}\right)^{1/2} \tanh[\sigma\epsilon\phi Z(\nu_v + \nu_i)t]^{1/2} . \quad (8)$$

Consequently, as already indicated,[20] the buildup profile, until a quasistationary concentration is reached, is defined by three parameters:

the initial slope,

$$\left.\frac{\partial c}{\partial t}\right|_0 = \sigma\epsilon\phi , \quad (9)$$

the asymptotic level,

$$c_{qst} = [\sigma\epsilon\phi / Z(\nu_v + \nu_i)]^{1/2} , \quad (10)$$

a characteristic time t^*, which corresponds to a fraction $(e-1)/(e+1) = 0.462$ of the asymptotic concentration. It is given by

$$t^* = [4\sigma\epsilon\phi Z(\nu_v + \nu_i)]^{-1/2} . \quad (11)$$

The ratio of these three parameters, two by two, gives

$$\left.\frac{\partial c}{\partial t}\right|_0 \Big/ (c_{qst})^2 = 1/4 \left.\frac{\partial c}{\partial t}\right|_0 (t^*)^2 = \frac{1}{2t^* c_{qst}} = Z(\nu_i + \nu_v) . \quad (12)$$

Another possible experimental approach to Z is provided by the consideration of the elimination kinetics of the defect supersaturation, which occurs when the irradiation is stopped. A bimolecular reaction takes place, with two species continuously in equal number, which gives rise to a second-order kinetics. The relevant equation, as derived from Eq. (7), is written

$$\frac{\partial c}{\partial t} = -Z c^2 (\nu_v + \nu_i) . \quad (13)$$

Hence

$$\frac{1}{c} = Z(\nu_s + \nu_f)t + \frac{1}{c(0)} . \quad (14)$$

Thus an analysis of the decay of the defect populations after suppression of flux enables another determination of the Z parameter, independently of its measurement during irradiation.

In either case, the desired information about the dynamic defect concentrations involved can be gained—in ordering alloys—by the measurement of the rate at which directional order is established as a result of an applied stress (Zener relaxation). This rate is related to the instantaneous concentrations, c_j, and the mean rates, ν_j^*, at which atom-defect interchanges occur by[23]

$$\tau^{-1} = \sum_j \alpha_j c_j \nu_j^* , \quad (15)$$

where the α's are efficiency factors and

$$\nu_j^* = \nu_{0j}^* \exp\left(-\frac{E_j^*}{kT}\right) . \quad (16)$$

Effective jump rates, ν^*, are distinguished from defect mobilities, ν, to take into account the fact that not all atom jumps are equally efficient in producing directional order.[24,25] Transposition of expressions (9), (10), and (11) to the ordering rate leads to the following formulas:

$$\left.\frac{\partial \tau^{-1}}{\partial t}\right|_0 = (\alpha_v \nu_v^* + \alpha_i \nu_i^*)\sigma\epsilon\phi , \quad (17)$$

$$\tau_{qst}^{-1}=(\alpha_v\nu_v^*+\alpha_i\nu_i^*)[\sigma\epsilon\phi/Z(\nu_v+\nu_i)]^{1/2}, \quad (18)$$

while t^* is kept unchanged. Comparison of the three parameters yields a coherency relation:

$$2t^*\left.\frac{\partial\tau^{-1}}{\partial t}\right|_0=\tau_{qst}^{-1} \quad (19)$$

Now the ratios of these parameters, two by two, bring us to define a new parameter, R, such that

$$R=\left.\frac{\partial\tau^{-1}}{\partial t}\right|_0\Big/(\tau_{qst}^{-1})^2=1\Big/4\left.\frac{\partial\tau^{-1}}{\partial t}\right|_0(t^*)^2$$
$$=\frac{1}{2t^*\tau_{qst}^{-1}}$$
$$=\frac{Z(\nu_v+\nu_i)}{\alpha_v\nu_v^*+\alpha_i\nu_i^*}. \quad (20)$$

Similarly, the decay kinetics after flux is suppressed is governed by the same parameter, since Eq. (14) leads to

$$\tau(t)=\frac{Z(\nu_v+\nu_i)}{\alpha_v\nu_v^*+\alpha_i\nu_i^*}t+\tau(0), \quad (21)$$

that is,

$$\tau(t)=Rt+\tau(0). \quad (22)$$

In summary, anelasticity studies of the ordering rate in appropriate alloys open access to three independent measurements of the recombination factor R. Derivation of the spontaneous recombination radius is then obtained by simple use of expression (6). It appears from the examination of expressions (20) and (21) that accurate information about the mobility parameters and ordering efficiencies in the material considered is required for a proper determination of r_v to be made. From prior quenching and irradiation work,[26-28] this requirement seems to be adequately satisfied in a series of concentrated Ag-Zn solid solutions. Further, it was shown that the dislocation sink density in alloys of this system could be reduced to an extremely low level such that equations for pure recombination apply validly. Owing to these highly favorable conditions, this alloy system was selected for the present investigation of the recombination efficiency to be made.

III. EXPERIMENTAL CONDITIONS

The material was an Ag-30 at.% Zn alloy prepared by melting in a quartz tube under vacuum the required amounts of 6 N Cominco Ag and 6 N 5 Zn supplied by the Laboratoire d' Electronique et de Technologie de l' Informatique du Centre d' Etudes Nucléaires de Grenoble. The specimens were strips 250 μm×2 mm×10 mm obtained by cold rolling. They were given a five-day anneal at 700 °C under vacuum followed by a slow cooling. This treatment was to produce proper homogenization, together with a large grain size and a low dislocation density.

The experimental procedure has been reported elsewhere.[20] At appropriate times in the irradiation schedule, a change in the state of stress is applied to the specimen which is initially in elastic equilibrium and the resulting strain is measured as a function of time. The anelastic strain relaxation is then analyzed by methods described in the literature.[26]

The in-flux study was done with the measuring device, an inverted torsion pendulum with negligible inertia, working in line with a Van de Graaf accelerator, in a constant flux for beam intensities in the range 1×10^9 to 4×10^{12} $e^-\,cm^{-2}\,sec^{-1}$. The corresponding defect production rates are extremely small. They are ranging between 6×10^{-14} and 3×10^{-10} displacement per atom per second. Irradiation temperatures were between −70 and +140 °C. The induced defect concentrations were of the order of 10^{-6} to 10^{-10} at.$^{-1}$.

IV. RESULTS

The whole study has been conducted in conditions of predominant recombination as was verified earlier.[20,27] A typical buildup profile on application of flux is shown in Fig. 1.

A. Flux dependence of the buildup parameters

The recombination factor R was obtained first by following the buildup profile for the rate curve on application of flux. The three parameters which characterize the evolution of the relaxation rate until a quasistationary maximum is reached were derived. This study was conducted at 20 °C in a wide range of instantaneous fluxes, which covers three decades. The corresponding experimental values for the initial slope of the rate curve, the characteristic buildup time, and the relaxation rate at the quasistationary maximum are given in Table I.

The associated quantities $(\partial\tau^{-1}/\partial t)_0$, $(2t^*)^{-2}$, and $(\tau_{qst}^{-1})^2$, which appear in expression (20), have been reported in Fig. 2. The respective data points fit well the straight lines traced with a slope equal to unity. This connotes that all three parameters vary proportionally to flux in agreement with theory. An interesting point is that the intermediate straight line is equidistant from the extreme ones in conformity with the coherency relation, Eq. (20). Further, the affinity ratio necessary to shift one line into coincidence to the next is found to be 18. According to relation (20), this is a measure of R. In fact only two of the three above-mentioned approaches to R are independent determinations of this parameter.

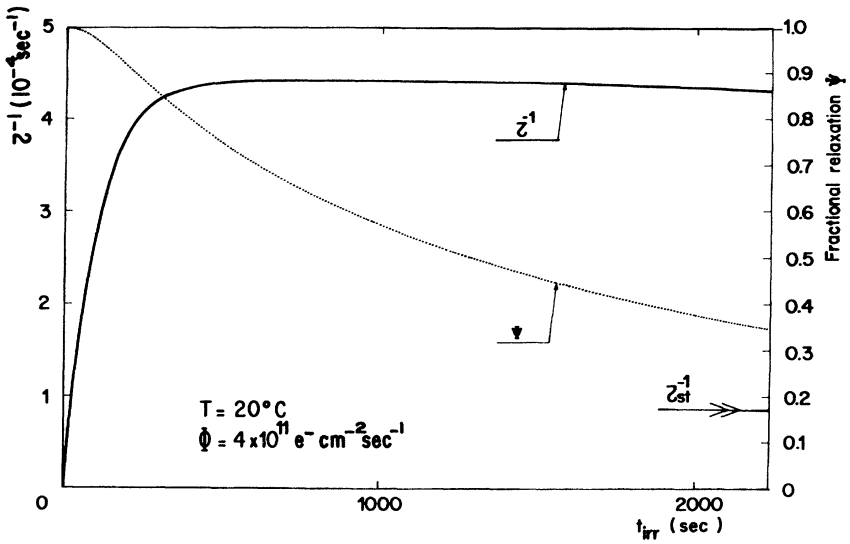

FIG. 1. Typical buildup profile in a Ag-30 at.% Zn alloy exposed to electron irradiation in a constant flux of 4×10^{11} $e^-cm^{-2}sec^{-1}$ (Ref. 20). Both the fractional anelastic relaxation (right scale) and the derived evolution of the relaxation rate are given as a function of the irradiation time at a temperature of 20 °C. The representation of these curves has been restricted to times up to 2200 sec. For longer irradiation periods only the asymptotic value is indicated. It should be reached after about 10^7 sec.

B. Temperature dependence of the buildup parameters

The same analytical parameters have been studied as a function of temperature (Table II). Figure 3 is an Arrhenius plot for the corresponding quantities which enter in expression (20). It can be seen that, within the limits of the intermediate and high irradiation temperatures, the data points are well aligned along three parallel straight lines. The physical meaning of the observed common slope is one-half the activation energy for the faster moving radiation-created defect in the alloy.[20] The two extreme lines are equidistant from the central one as predicted by relation (20). Again a common value of 18 is found for the affinity ratio from one line to the next; that is exactly the same as derived above from the flux dependence study at 20 °C. Thus in the considered temperature range the recombination efficiency is temperature independent as a first approximation.

This conclusion holds only for temperature higher than about −10 °C. At lower temperatures significant deviations to linearity occur for the char-

TABLE I. Determination of the parameters which define the relaxation rate versus irradiation time curve for different instantaneous electron fluxes at a constant temperature of 20 °C. The fifth column is to verify that the coherency relation required for the pure recombination case is correctly satisfied. The three last columns on the right indicate the values which are derived for the recombination factor R. Averages for each column are respectively 19, 17, and 18 yielding an overall average of 18.

Flux rate	Analytical parameters			Coherency	Recombination factor R		
ϕ ($e^-cm^{-2}sec^{-1}$)	$\left.\frac{\partial\tau^{-1}}{\partial t}\right\|_0$ (sec^{-2})	t^* (sec)	τ_{qst}^{-1} (sec^{-1})	$\frac{2t^*\left.\frac{\partial\tau^{-1}}{\partial t}\right\|_0}{\tau_{qst}^{-1}}$	$\frac{\left.\frac{\partial\tau^{-1}}{\partial t}\right\|_0}{(\tau_{qst}^{-1})^2}$	$\frac{1}{4\left.\frac{\partial\tau^{-1}}{\partial t}\right\|_0 t^{*2}}$	$\frac{1}{2t^*\tau_{qst}^{-1}}$
4×10^{12}	3.6×10^{-5}	20	1.5×10^{-3}	1.0	16	17	17
1.2×10^{12}	8.4×10^{-6}	45	7.0×10^{-4}	1.1	17	15	16
4×10^{11}	3.4×10^{-6}	65	4.2×10^{-4}	1.0	19	17	18
1.2×10^{11}	9.5×10^{-7}	130	2.4×10^{-4}	1.0	16	16	16
4×10^{10}	3.8×10^{-7}	200	1.4×10^{-4}	1.1	19	16	16
1.2×10^{10}	7.6×10^{-8}	420	6.7×10^{-5}	1.0	17	19	18
4×10^{9}	4.5×10^{-8}	590	4.0×10^{-5}	1.3	28	16	21
1.2×10^{9}	8.3×10^{-9}	1270	2.0×10^{-5}	1.1	21	19	20

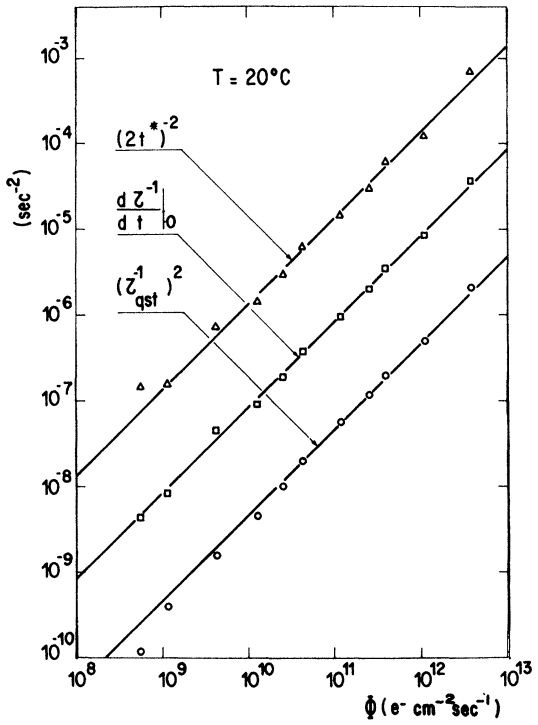

FIG. 2. Flux dependence of the initial slope, characteristic time, and quasistationary relaxation rate at a constant temperature of 20 °C. The straight lines have been traced with a slope equal to unity.

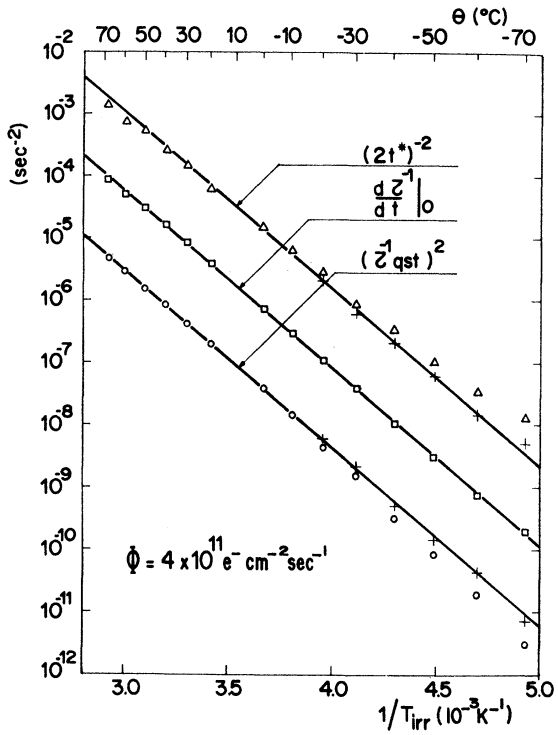

FIG. 3. Temperature dependence of the initial slope, characteristic time, and quasistationary relaxation rate. The flux rate was 4×10^{11} e^-cm^{-2}sec^{-1}. △, ○, and □ are uncorrected data points. The meaning of the crosses is discussed in the text.

acteristic time and the quasistationary relaxation rate. They reflect a marked increase of the effective recombination efficiency when temperature is decreased. This point will be discussed in some detail in the following section.

C. Elimination kinetics of the defect supersaturation on suppression of flux

Figure 4 illustrates the pattern of the relaxation evolution which was observed when flux was sup-

TABLE II. Experimental values of the parameters which describe the relaxation rate versus irradiation time curve for different temperatures in a constant flux of 4×10^{11} e^-cm^{-2}sec^{-1}. The last four columns indicate the inferred recombination factor R.

Temperature	Analytical parameters			Coherency	Recombination factor R			
(°C)	$\frac{\partial \tau^{-1}}{\partial t}\Big|_0$ (sec^{-2})	t^* (sec)	τ^{-1}_{qst} (sec^{-1})	$\frac{2t^* \frac{\partial \tau^{-1}}{\partial t}\Big|_0}{\tau^{-1}_{qst}}$	$\frac{\frac{\partial \tau^{-1}}{\partial t}\Big|_0}{(\tau^{-1}_{qst})^2}$	$\frac{1}{4\frac{\partial \tau^{-1}}{\partial t}\Big|_0 t^{*2}}$	$\frac{1}{2t^*\tau^{-1}_{qst}}$	Average
70	8.7×10^{-5}	13	2.2×10^{-3}	1.0	18	17	17	18
60	5.0×10^{-5}	19	1.7×10^{-3}	1.1	17	14	16	18
50	3.0×10^{-5}	21	1.2×10^{-3}	1.0	21	19	20	18
40	1.6×10^{-5}	31	9.2×10^{-4}	1.1	19	16	18	18
30	8.6×10^{-6}	41	6.4×10^{-4}	1.1	21	17	19	18
20	3.4×10^{-6}	65	4.2×10^{-4}	1.1	19	17	18	18
0	7.4×10^{-7}	130	2.0×10^{-4}	1.0	18	20	19	18
−10	3.0×10^{-7}	195	1.2×10^{-4}	1.0	21	22	21	21
−20	1.1×10^{-7}	300	6.6×10^{-5}	1.0	25	25	25	25
−30	4.0×10^{-8}	530	4.0×10^{-5}	1.1	25	22	24	23
−40	1.1×10^{-8}	855	1.8×10^{-5}	1.0	34	31	32	32
−50	3.2×10^{-9}	1520	9.3×10^{-6}	1.0	37	34	35	35
−60	7.6×10^{-10}	2655	4.4×10^{-6}	0.9	39	47	43	43
−70	2.0×10^{-10}	4290	1.8×10^{-6}	1.0	62	68	65	65

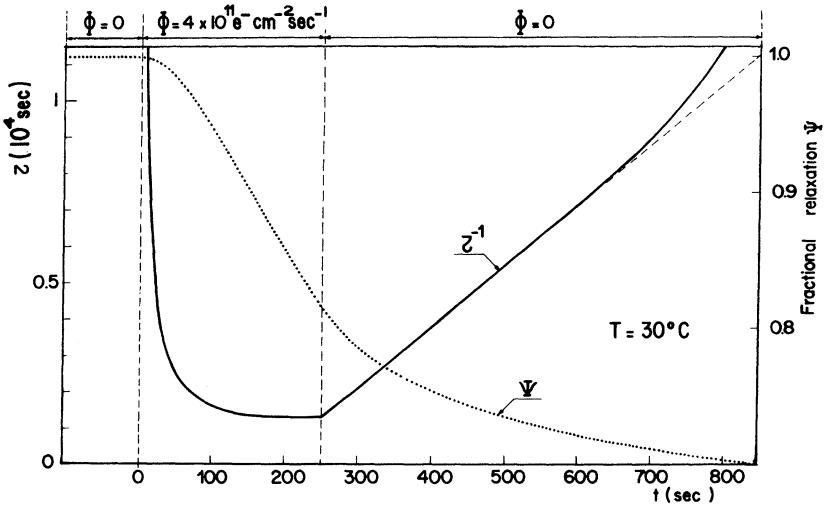

FIG. 4. Evolution of the relaxation time τ after suppression of flux in the quasistationary regime. Flux was first applied during a period long enough to reach the quasistationary regime, namely, 250 sec. Irradiation was then stopped, to follow the decay of the enhanced relaxation rate.

pressed once the quasistationary state was reached. In conformity with expression (21), the characteristic relaxation time, τ, increases linearly with the time elapsed after the irradiation was stopped.

This type of study has been conducted at several temperatures. Figure 5 shows a series of curves traced at temperatures between −60 and +80 °C. It can be seen that all curves exhibit a straight variation over a large portion of the evolution of τ. Further, at least between 0 and 80 °C, the slope of the straight lines does not depend on temperature to a first approximation. This agrees with the model predictions for the case when defect elimination is predominantly recombination, expression (21) (with the assumption that $\alpha_v \simeq \alpha_i$ and $\nu^* \simeq \nu$). For the case when defects would get eliminated on fixed sinks, it can be readily shown that this slope would increase proportionally to ν_f. This would lead to a marked temperature dependence which is definitely not observed experimentally. However, a temperature dependence appears but only in the lower temperature region. It cannot originate in this cause. First, at lower temperatures, owing to increased defect concentration, conditions for pure recombination are much more easily satisfied. Second, the observed variation is an increase for decreasing temperatures instead of a decrease. The possible physical reasons for this variation will be discussed below.

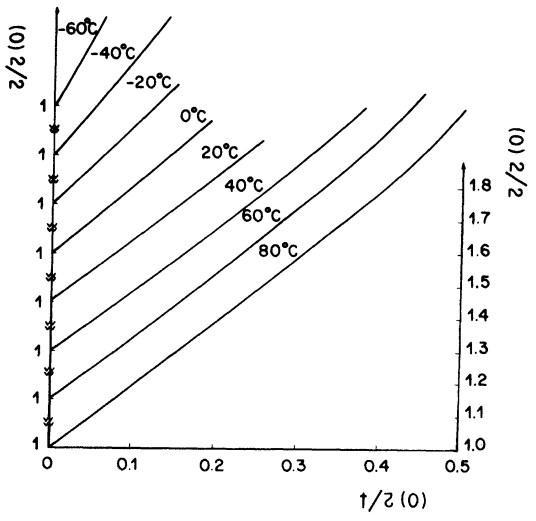

FIG. 5. Influence of temperature on the variation law of the relaxation time as a function of the time elapsed after suppression of flux. The experimental sequence precluding this evolution has been presented in Fig. 4. All measurements have been conducted after irradiations at a flux rate of 4×10^{11} $e^-cm^{-2}sec^{-1}$.

V. DISCUSSION

A. Analysis and interpretation of the recombination parameters studied

As readily derived by combination of expressions (6) and (20) or (21), the spontaneous recombination radius r_v is connected to the measured recombination factor R by

$$R = \frac{2\pi\sqrt{2}}{3} r_v \frac{\nu_v + \nu_i}{\alpha_v \nu_v^* + \alpha_i \nu_i^*} \tag{23}$$

in units of interatomic distances. Figure 6 is to sum up all the r_v values deduced from this relation assuming $\alpha_v = \alpha_i$, $\nu_v^* = \nu_v$, and $\nu_i^* = \nu_i$. It can be seen that the three independent approaches to R yield values in satisfactory agreement. Further, all three curves exhibit in common a marked temperature dependence.

To better approximate r_v, the α and ν parameters must be known. In previous work the relevant α parameters have been determined to be both of the order of, but less than, unity.[28] The effective jump rates ν^* are themselves slightly smaller than the defect mobilities ν (see Appendix). Consequently the calculated r_v values reported in Fig. 6 are by excess. Thus, it can be concluded that, in the temperature range above 0 °C, the capture radius is about (or possibly a little smaller than) six interatomic distances. This is the commonly accepted order of magnitude for a metal lattice.

However, it is to be noted that the recombination parameters which were derived from the present experiments are appropriate and valid for macroscopic descriptions of the recombination process only, while for a more detailed insight at a microscopic scale a mathematical treatment is needed. In fact several approaches have been proposed to evaluate the reaction kinetics relevant to the mutual annihilation of vacancies and self-interstitials in a metal lattice and infer the interaction range and capture radius for these species, namely, continuum approaches based on use of rate or diffusion equations[21,29] on one hand and Monte Carlo methods, on the other hand.[30-34] In the latter cases, statistical fluctuations in the defect distributions are taken into account as well as the detailed atomistic features for the recombination volume. The common result to all these treatments is that they yield second-order kinetics in the limit of low defect concentrations. Waite's theoretical description model of the diffusional point-defect flow into randomly distributed *spherical* sinks of radius r gives the following equation featuring the time evolution of the concentration of the mobile defects for a random initial distribution:

$$\frac{1}{c} - \frac{1}{c_0} = \tfrac{4}{3}\pi \frac{r}{a} n + 32\left(\frac{\pi}{12}\right)^{1/2}\left(\frac{r}{a}\right)^2 n^{1/2}. \qquad (24)$$

In this expression n is the average number of jumps for the mobile defects before elimination. For large n this expression yields the already mentioned linear relation between the recombination efficiency and the "capture" radius r_v, expression (6). Clearly in this scheme the capture radius is a phenomenological parameter which is not evaluated by the model calculation. By contrast, reaction constants can in principle be determined directly with Monte Carlo simulations using microscopic interaction criteria. An interesting example is provided by Fastenau's treatment of a cloud random walk.[33] Indicatively the effective recombination radius appears to be about 1.5 interatomic distances for a cloud of 32 substitutional sites in an fcc lattice. Unfortunately, this type of calculation is restricted to capture entities of small size due to computer limitations.

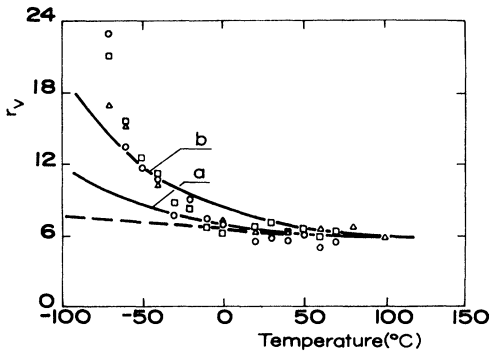

FIG. 6. Temperature dependence of the recombination radius r_v. Three independent measurements were performed, based on △ recovery studies after suppression of flux; ○ comparison of the buildup parameters, initial slope, and characteristic time, on application of flux; □ comparison of the initial ordering rate on application of flux and the quasistationary rate. The results are expressed in units of interatomic distances. The dashed curve is to illustrate the $T^{-1/3}$ dependence predicted by theory. Curves *a* and *b* are for the case when the activation energies for directional ordering and for vacancy migration differ by 0.02 and 0.04 eV, respectively.

B. The temperature dependence of the recombination radius

As already indicated, the interaction distance between an interstitial and a vacancy is expected to be temperature dependent and to be progressively decreased when temperature is increased.[1] This temperature dependence is not easily estimated since it implies the choice of a realistic potential and the solution of the general diffusion equations in the presence of a drift term associated with the existence of a long-range interaction potential. Calculations of this type indicate that the interaction radius can be written[2,3]

$$r_v = \left(\frac{Q}{kT}\right)^{1/n}, \qquad (25)$$

where Q and n are constants. The value generally proposed for n is three. It connotes an interaction of elastic origin.

By contrast, a much stronger temperature dependence is revealed in Fig. 6 for the Ag-30 at. % Zn alloy investigated presently. For a proper

interpretation to be made, a detailed analysis of the factors which might influence this result is required. First, Eq. (23) is to be examined. At the low temperatures for which R is rapidly increasing, the defect mobilities ν_i and ν_v are markedly differentiated. What is more, the existing data indicate unambiguously that $\nu_i \ll \nu_v$,[27,28] such that expression (23) is restricted to

$$R \simeq \frac{2\pi\sqrt{2}}{3} r_v \frac{\nu_v}{\alpha_v \nu_v^*} . \tag{26}$$

Then it appears that the observed variation of R with temperature, Fig. 6, can be due to a difference in the activation energies for directional ordering and for vacancy migration. However, as indicated in the Appendix, this difference, if any, is smaller than 0.04 eV. Its possible incidence on the $R(T)$ law is featured in Fig. 6. It can be seen that no satisfactory fit to the experimental profile can be obtained. A difference smaller than 0.02 eV is compatible with the data but in a range restricted to temperatures higher than −20 °C. It can in no way explain the drastic increase observed on the low-temperature side.

Interpretation of the results can be tentatively provided by consideration of the possible formation, under particular temperature conditions, of a different defect species (referred to hereafter by f), with mobility higher than the one for single vacancies. Then the recombination factor R would be proportional to

$$(\nu_v + \nu_f)/(\alpha_v \nu_v^* + \alpha_f \nu_f^*) ,$$

with $\nu_f \gg \nu_v$ and $\nu_f^* \gg \nu_v^*$. Furthermore, if these defects have low efficiency in promoting ordering, that is, if $\alpha_f \simeq 0$, R would tend to large values. Such a situation potentially exists at temperatures when crowdions are stable. However, in this scheme, the experimentally observed effect would imply the conversion temperature for these defects to be about 200 K. An alternate explanation is that divacancies are formed as a result of the vacancy concentrations being increased rapidly when temperature is lowered. Unfortunately, information is lacking about the mobility of divacancies and their eventual contribution to ordering in AgZn and other concentrated alloys as well. Specific quench studies are required for this sort of interpretation to be confirmed.

To close, it is recalled that a similar behavior has been observed by Poerschke and Wollenberger[16] in a Cu-59 at. % Ni alloy, in which the capture radius r_v showed a drastic increase at temperatures around 150 K as indicated in Fig. 7. The temperature dependence observed in this case would indicate an interaction energy inversely proportional to r, the separation distance between interstitial and vacancy, instead of the $1/r^3$ variation predicted for an elastic interaction.

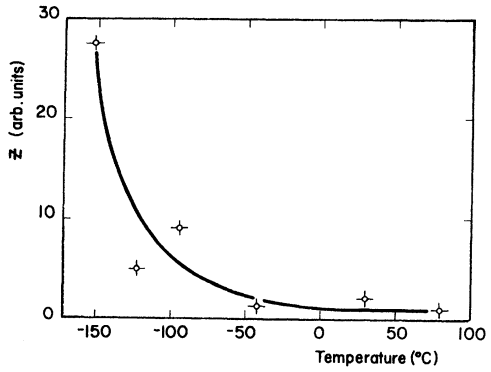

FIG. 7. Temperature dependence of the recombination radius r_v observed in an Cu-59 at. % Ni [after Poerschke and Wollenberger (Ref. 6)].

VI. SUMMARY

The reaction constants for the interaction between vacancies and self-interstitials could be determined in an Ag-30 at. % Zn alloy directly during irradiation with fast electrons at high temperatures, that is, in conditions of a dynamic regime when both created defect species migrate freely. The recombination efficiency which was measured yielded a value of about six interatomic distances for the spontaneous capture radius in the temperature range between 270 and 370 K. The same result was derived from an independent determination based on analysis of the decay of the defect populations on suppression of flux. Clearly, the capture radius in the concentrated alloys studied is comparable to the ones generally found in pure or doped metals.

Similar experiments were conducted at lower temperatures, down to 200 K. They indicated a rapid enhancement of the recombination efficiency, but this effect might be due to the occurrence of complex reactions between point defects resulting in the formation of highly mobile multiple vacancies. More work is needed to examine further this effect and its possible incidence on the effective recombination parameters for the elemental defects.

To sum up, anelasticity experiments conducted in conditions of permanent irradiation enable detailed analysis of the capture radius between vacancies and self-interstitials in concentrated alloys. The interesting feature of this new approach to recombination reactions is that it can be applied to a wide temperature region above stage III of irradiated metals; thus it appears to complement previous studies of the recombination volume in metallic materials.

ACKNOWLEDGMENTS

The authors wish to express their thanks to Professor W. Frank, Professor P. Lucasson, and Professor A. Seeger for helpful discussions. Dr. O. Dimitrov, P. Vajda, and U. Goesele are gratefully acknowledged for valuable suggestions.

APPENDIX: DIRECTIONAL ORDERING RATE IN RELATION TO VACANCY JUMP FREQUENCY

Under nonequilibrium conditions, the vacancy mobility influences the directional ordering rate at two levels. First it controls the vacancy lifetime and hence the instaneous defect concentration after a given thermal or irradiation sequence. In this respect, although the vacancy is able to make exchange jumps alternately with the two types of constituent atoms in the binary alloy, it is unnecessary to distinguish between the two types of jumps. Consequently the vacancy mobility ν_v, in the sense of the mean diffusional rate towards sinks and of the relevant lifetime is adequately defined by the usual expression

$$\nu_v = Z_c \nu_D \exp\left(\frac{S_v^M}{k}\right)\exp\left(-\frac{E_v^M}{kT}\right),$$

where Z_c is the coordination number, ν_D the Debye frequency, and E_v^M the vacancy migration energy. On the contrary not all atom jumps are equally efficient in promoting directional order. In particular a vacancy which would be systematically exchanged with atoms of one single type would not contribute to the ordering process. To take this physical fact into account, a weighed frequency ν^* can be used as defined by

$$\frac{2}{\nu^*} = k\left(\frac{1}{\nu_A} + \frac{1}{\nu_B}\right),$$

where k is a constant, and ν_A and ν_B are the jump frequencies for the A and B atoms, respectively. The activation energy E^* associated to mobility ν^* is simply

$$E_v^* = \frac{\partial}{\partial(1/kT)} \ln\left(\frac{1}{\nu_A} + \frac{1}{\nu_B}\right).$$

Thus ν^* and E^* are parameters which enable a phenomenological description of the ordering kinetics. Now if the vacancies only are considered, their mobility ν_v is simply the sum $\nu_A + \nu_B$. Hence

$$E_v^M = \frac{\partial}{\partial(1/kT)} \ln\left(\frac{1}{\nu_A} + \frac{1}{\nu_B}\right).$$

Clearly if ν_A is different from ν_B, the lifetime is determined by the faster jump, while the ordering rate is controlled rather by the slower jump. The frequencies ν_A and ν_B are connected to the diffusion coefficients D_A^* and D_B^* for the corresponding radioactive tracers in the alloy by[22]

$$D_A^* = \frac{c_v \nu_A a^2}{c_A} \quad \text{and} \quad D_B^* = \frac{c_v \nu_B a^2}{c_B}.$$

Some data about the above parameters are available is concentrated α-AgZn solid solutions. For the 30 at.% Zn composition, diffusion experiments in the range 500 to 700 °C yielded $D_{Ag}^* = 0.29 \exp(-1.56\ \text{eV}/kT)$ and $D_{Zn}^* = 0.46 \exp(-1.53\ \text{eV}/kT)\ \text{cm}^2\,\text{sec}^{-1}$.[35] Thus the measured activation energies for the two constituent elements are very close, which suggests that E_v^M and E_v^* differ but slightly. This was confirmed by anelasticity measurements in the quenched state, in which E_v^* and E_v^M were determined to be 0.54 ± 0.02 and 0.52 ± 0.04 eV, respectively.[26,27] It is to be noted that a similar behavior was observed in an AgZn alloy of neighbor composition, Ag-24 at.% Zn, in which the corresponding values were found to be 0.56 ± 0.02 and 0.51 eV (with lower accuracy), respectively.[26] Thus it can be concluded that in the concentrated alloys under consideration the difference in the activation energies for directional ordering and for vacancy migration, if any, is very small.

---

*Permanent address: Ecole Nationale Supérieure de Céramique Industrielle, 47 rue Albert Thomas, 87100, Limoges, France.

[1] K. Schroeder and K. Dettman, Z. Phys. B22, 343 (1975).
[2] M. Profant and H. Wollenberger, Phys. Status Solidi B 71, 515 (1975).
[3] M. H. Yoo and W. H. Butler, Phys. Status Solidi B 77, 181 (1976).
[4] H. J. Wollenberger, *Vacancies and Interstitals in Metals* (North-Holland, Amsterdam, 1970), p. 215.
[5] G. Duesing, H. Hemmerich, W. Sassin, and W. Schilling, *Proceedings of the International Conference on Vacancies and Self-Interstitials in Metals, Jülich, 1968* (Kernforschungsanlage, Jülich, Germany, 1968), Vol. I, p. 246.
[6] J. A. Horak and T. H. Blewitt, Phys. Status Solidi A 9, 721 (1972).
[7] P. Vajda and M. Biget, Phys. Status Solidi A 23, 251 (1974).
[8] O. Dimitrov, C. Dimitrov, P. Rosner, and K. Böning, Radiat. Eff. 30, 135 (1976).
[9] W. Schilling, G. Burger, K. Isebeck, and H. Wenzl, *Vacancies and Interstitials in Metals* (North-Holland, Amsterdam, 1970), p. 255.
[10] K. Schroeder, Radiat. Eff. 5, 255 (1970).
[11] F. Dworschak, E. Schnoter, H. Wollenberger, and J. Wurm, Phys. Status Solidi 29, 75 (1968); 29, 81 (1968).

[12]F. Dworschak, R. Lennartz, T. Monsau, and H. Wollenberger, Proc. Int. Conf. on Fund. Aspects of Rad. Damage in Metals, Gatlinburg, USA, p. 601, 1975.
[13]F. Dworschak, H. E. Schepp, and M. Wollenberger, Appl. Phys. 46, 1049 (1975).
[14]R. Lennartz, F. Dworschak, and H. Wollenberger, J. Phys. F 7, 2011 (1977).
[15]K. Schroeder and W. Heidrich, Phys. Lett. 43A, 315 (1973).
[16]R. Poerschke and H. Wollenberger, J. Phys. F 6, 27 (1976).
[17]D. E. Becker, F. Dworschak, and H. Wollenberger, Phys. Status Solidi B 54, 455 (1972).
[18]A. C. Damask, Acta Metall. 13, 1104 (1965).
[19]G. J. Dienes and A. C. Damask, J. Appl. Phys. 29, 1713 (1958).
[20]M. Halbwachs, J. Phys. F 8, 6 (1978).
[21]T. R. Waite, Phys. Rev. 107, 463 (1957).
[22]Y. Adda and J. Philibert, *La diffusion dans les solides* (Presses Universitaires de France, Paris, 1966), p. 24 and 159.
[23]A. S. Nowick and B. S. Berry, *Anelastic Relaxation in Crystalline Solids* (Academic, New York, 1972), Chap. X.
[24]S. Radelaar, in *Proceedings of the International Conference on Vacancies and Self-Interstitials in Metals, Julich, 1968* (Kernforschungsanlage, Jülich, Germany, 1968), Vol. II, p. 667.
[25]A. Caplain and W. Chambron, Acta. Metall. 25, 1001 (1977).
[26]B. S. Berry and J. L. Orehotsky, Acta Metall. 16, 683 (1968); 16, 697 (1968).
[27]M. Halbwachs and J. Hillairet, Phys. Rev. B 18, 4927 (1978).
[28]M. Halbwachs, J. T. Stanley, and J. Hillairet, Phys. Rev. B 18, 4938 (1978).
[29]F. S. Ham, J. Appl. Phys. 30, 915 (1959).
[30]H. Mehrer, Z. Naturforsch. 24A, 358 (1969).
[31]P. Streda, Cryst. Lattice Defects 1, 229 (1970).
[32]R. H. J. Fastenau, A. van Veen, P. Penning, and L. M. Caspers, Phys. Status Solidi A 47, 577 (1978).
[33]R. H. J. Fastenau, Phys. Status Solidi A 53, K39 (1979).
[34]R. H. J. Fastenau, C. M. van Baal, P. Penning, and A. van Veen, Phys. Status Solidi A 52, 577 (1979).
[35]D. Lazarus and C. T. Tomizuka, Phys. Rev. 103, 1155 (1956).